Biochemical and Biophysical Research Communications 520 (2019) 466–472

Contents lists available at ScienceDirect

Biochemical and Biophysical Research Communications

journal homepage: www.elsevier.com/locate/ybbrc

Structural analysis of human sterol transfer protein STARD4

Lingchen Tan [1], Junsen Tong [1], ChangJu Chun**, Young Jun Im*

College of Pharmacy, Chonnam National University, 77 Yongbong-ro, Buk-gu, Gwangju, 61186, South Korea

ARTICLE INFO

Article history:
Received 29 September 2019
Accepted 4 October 2019
Available online 11 October 2019

Keywords:
Protein structure
STARD4
Sterol transport
Lipid transfer protein
Liposome
Cholesterol

ABSTRACT

The steroidogenic acute regulatory protein (StAR)-related lipid transfer domain-4 (STARD4) is a sterol-binding protein that is involved in cholesterol homeostasis by intracellular sterol transport. In this work, we determined the crystal structures of human STARD4 and its Ω1-loop mutant in apo forms at 1.95 and 1.7 Å resolutions, respectively. The structure of human STARD4 displays a conserved α-helix/β-grip fold containing a deep hydrophobic pocket. The Ω1-loop which serves as a lid for the hydrophobic pocket has a closed conformation. The shape of the sterol-binding cavity in the closed form is not complementary to accommodate cholesterol, suggesting that a conformational change of the Ω1-loop is essential for sterol binding. The human STARD4 displayed sterol transfer activity between liposomes, and the mutations in the Ω1-loop and the hydrophobic wall abolished the transfer activity. This study confirms the structural conservation of the STARD4 subfamily proteins and the flexibility of the Ω1-loop and helix α4 required for sterol transport.

1. Introduction

Cholesterol is one of the major components in eukaryotic cellular membranes and the concentration of sterol within the membrane varies widely between organelles [1]. Sterols determine the physicochemical properties of lipid bilayer and regulate the functioning of membrane proteins. The endoplasmic reticulum (ER) synthesizes cholesterol but contains only 0.5–1% of total cellular cholesterol. The majority of cellular cholesterol up to 60–80% was estimated to present in the plasma membrane [2], implying the presence of efficient sterol transport pathways between organellar membranes. Due to the poor solubility in water, sterols cannot diffuse between the membrane compartments separated by an aqueous phase. Various transport processes contribute to the intracellular sterol distribution, but nonvesicular transport involving soluble lipid transfer proteins (LTPs) accounts 70% of cholesterol transport [3]. Non-vesicular sterol transport is mainly carried out by three families of LTPs including ORP (oxysterol-binding protein-related protein), StART (steroidogenic acute regulatory protein-related transfer protein), and LAM (LTP anchored at a membrane contact site) [4].

In humans, there are fifteen StART-related domain (STARD) proteins and they are subdivided into six subfamilies [5,6]. Owing to their variation in binding cavities, STARD proteins recognize various lipid types such as phosphatidylcholine, phosphatidylethanolamine, sterols, and ceramides [5]. STARD1 (STARD1/3) and STARD4 (STARD4/5/6) subfamilies are known to bind sterol [7–9] and are implicated in maintaining cholesterol homeostasis by intracellular sterol transport [10]. The members of the STARD4 subfamily are composed of a single sterol-binding domain with α-helix/β-grip fold of approximately 210 amino acids and do not contain the N-terminal targeting modules. Their cellular localization is cytoplasmic, but they have some interaction with organelles such as the ER and endocytic recycling compartment (ERC) [10]. STARD4 takes up a sterol in the hydrophobic cavity and diffuses through the cytoplasm, and it is thought to provide many subcellular organelles such as ER, endosome and lysosomes, with cholesterol [11]. STARD4 is expressed in many tissues with highest expression in liver and kidney [11]. STARD4 accounts for large fraction of sterol transport between the plasma membrane and the ERC [3]. In addition, STARD4 and STARD5 are known to stimulate steroidogenesis by facilitating the delivery of cholesterol from the outer to the inner mitochondrial membrane [6].

Despite the extensive studies on the STARD family proteins regarding biological function and transport mechanism, the key determinants for the ligand specificity and the mechanism of sterol uptake and release are still elusive. Recent structural studies on the

* Corresponding author.
** Corresponding author.
E-mail addresses: cchun1130@jnu.ac.kr (C. Chun), imyoungjun@jnu.ac.kr (Y.J. Im).
[1] These authors equally contributed to this work.

https://doi.org/10.1016/j.bbrc.2019.10.054
0006-291X/

LAM proteins of the StARkin superfamily suggested that sterol binds the cavity close to the tunnel entrance with a partially open lid [12–14]. However, due to the sequence and structural differences from the LAM proteins, prediction of a ligand-binding mode for STARD4 is obscure.

In this study, to better understand the structural aspects of sterol binding by human STARD4, we determined the crystal structures of human STARD4 and its Ω1-loop mutant in apo forms at 1.95 and 1.7 Å resolutions, respectively. This study confirms a conserved structural α-helix/β-grip fold in human STARD4 family members. The narrow sterol-binding cavity in the closed form of STARD4 requires a conformational change of the Ω1-loop for ligand binding. The in vitro sterol transport assay suggested the hydrophobic residues in the Ω1-loop and the cavity are essential for sterol transport.

2. Materials and methods

2.1. Cloning, protein expression and purification

The cloned gene of human STARD4 (UniProt ID: Q96DR4) in pT7T3Pac vector (Clone ID: KU029028) was purchased from Korea Human Gene Bank (KRIBB, Daejeon, Republic of Korea). The DNA encoding the STARD4 (residues 2–205) was amplified by polymerase chain reaction (PCR) and was subcloned into the BamHI/XhoI site of the modified pHIS-2 vector, in which the original TEV protease cleavage site was modified to a thrombin cleavage site [15]. STARD4 was tagged with an N-terminal hexa-histidine followed by a thrombin protease cleavage site (LVPR/GS). The exposed Cys75 in the helix α3 was mutagenized to serine to eliminate oxidation of the cysteine residue. The Ω1-loop deletion mutant (Δ107-110) was prepared by replacing the four residues 107–110 (LWNI) with two glycine residues by PCR based mutagenesis.

Escherichia coli BL21(DE3) cells transformed with the plasmid encoding the human STARD4 were grown to an OD_{600} of 0.8 at 310 K in Luria-Bertani medium. Protein expression was induced by the addition of 0.25 mM isopropyl β-D-1-thiogalactopyranoside and the culture was incubated for 12 h at 293 K before harvesting the cells. Cells were resuspended in lysis buffer (2X PBS buffer supplemented with 30 mM imidazole) and lysed by sonication. After centrifugation, the supernatant containing the His-tagged STARD4 was applied to a Ni–NTA affinity column. The Ni–NTA column was thoroughly washed with the lysis buffer. The protein was eluted from the column using 0.1 M Tris–HCl pH 7.0, 0.3 M imidazole, 0.3 M NaCl. The eluate was concentrated to 10 mg/ml and the His-tag was cleaved by addition of thrombin protease. The protein was subjected to size exclusion chromatography on a Superdex 200 column (GE Healthcare) equilibrated with 20 mM Tris–HCl pH 7.5, 0.15 M NaCl. The fractions containing STARD4 were concentrated to 10 mg/ml for crystallization.

2.2. Crystallization and crystallographic analysis

Crystals of the STARD4 C75S were obtained in 0.1 M Bicine pH 9.0, 30% PEG 1000 by hanging-drop vapor diffusion method at 14 °C. The crystals of STARD4 C75S Δ107-110 were obtained in 0.1 M MES pH 6.0, 25% PEG 3350, 200 mM NaCl. The crystals were cryoprotected by transferring them into reservoir solution supplemented with an additional 10% PEG 1000 and were flash-cooled by immersion in liquid nitrogen. Diffraction data for the STARD4 crystals were collected at a wavelength of 0.97950 Å using an ADSC Q270 CCD detector on the 7A beamline at Pohang Light Source (PLS), Pohang Accelerator Laboratory. All data were processed and scaled using HKL-2000 (HKL Research Inc.) and handled with the CCP4 program suite. Molecular replacement was carried out with software Phaser using mouse STARD4 structure (PDB code: 1JSS). The structural model was built and refined using Coot and Phenix (Table 1).

2.3. Liposome preparation and sterol transfer assay

Neutral lipid DOPC (1, 2-dioleoyl-sn-glycero-3-phosphocholine) and Dansyl-PE (1,2-dioleoyl-sn-glycero-3-phosphoethanolamine-N-(5-dimethylamino-1-naphthalenesulfonyl)) were obtained from Avanti Polar Lipids. DHE (dehydroergosterol) were obtained from Sigma-Aldrich. The liposomes were prepared and sterol transfer assays were performed as described [12]. Lipids dissolved in chloroform or in ethanol were mixed at the desired molar ratio and incubated at 37 °C for 5 min, and the solvent was evaporated by nitrogen stream. Dried lipids were re-suspended in 50 mM HEPES pH 7.2, and 100 mM potassium acetate (HK buffer) by pipetting. Liposomes were prepared at a total lipid concentration of 1mM in 1 ml buffer. The hydrated lipid mixture was frozen and thawed five times using a water bath and cooled ethanol at −70 °C. The lipid mixture was extruded ten times through a 0.1 μm (pore size) polycarbonate filter. The liposomes were stored at 4 °C in the dark and used within three days. The donor and acceptor liposomes contained 10 mol% DHE and 2.5 mol% dansyl-PE, respectively. For each transfer assay, 25 μl donor liposomes and 25 μl acceptor liposomes were added to the buffer in a quartz cuvette with a final volume of 2 ml. The final lipid concentration of donor and acceptor liposomes was 25 μM. The fluorescence measurement was initiated with gentle stirring at 25 °C. After 320 s the purified protein was injected to the liposome mixture with the final concentration of 1 μM. The fluorescence at 525 nm with an excitation wavelength of 324 nm was monitored for 800 s, using an FP-6200 spectrofluorometer (JASCO).

3. Results

3.1. Overall structure of human STARD4

Human STARD4 is composed of a single sterol-binding domain with 205 amino acids. Human STARD4 shares 30% and 24% sequence identities (53% and 46% similarity) with human STARD5 and STARD6, respectively (Fig. 1A). The core sterol-binding domains of human and mouse STARD4 are highly conserved with 85% sequence identity. However, human STARD4 lacks the N-terminal 16 residue extension compared to mouse STARD4. We purified the full length human STARD4. The purified STARD4 was monomeric but was susceptible to oxidative dimerization due to the presence of exposed Cys75 when analyzed by size exclusion chromatography. Therefore, we introduced C75S mutation on human STARD4 for biochemical and crystallographic studies. We have crystallized and solved the structure of human STARD4 C75S at 1.95 Å resolution by molecular replacement using the structure of mouse STARD4 (PDB id: 1JSS) (Table 1). All residues except the N-terminal five residues were well-defined in the $2F_o$-F_c electron density maps (Fig. 1B). Human STARD4 is a single α/β domain with 10-stranded U-shaped β-sheet flanked by long α-helices (Fig. 1C). The sterol-binding pocket is located in the center of protein with the cavity volume of 642 $Å^3$, which is slightly larger than the volume of cholesterol (432 $Å^3$). The hydrophobic tunnel is composed of twenty hydrophobic residues, five charged residues, and seven polar residues (Fig. 2A). The hydrophilic residues, Ser131, Arg76, and Asp80 are located near the tunnel bottom. Arg76 and Asp80 make a salt bridge and form hydrogen bond networks with the water molecules in the cavity. The one end of hydrophobic tunnel is closed by the ten residue β5-β6 loop (the Ω1-loop), which serves as a lid for the binding pocket [7,16].

Table 1
Data-collection and refinement statistics.

Crystal	STARD4 C75S	STARD4 C75S Δ107-110
Data collection		
Beamline	PLS-7A	PLS-5C
Wavelength (Å)	0.97950	0.97950
Space group	$P4_1$	$P2_12_12_1$
Unit-cell parameters (Å, °)	$a = 93.8$, $b = 93.8$, $c = 73.3$	$a = 42.9$, $b = 43.4$, $c = 89.8$
Resolution range (Å)	50–1.95 (1.98–1.95)	50–1.7 (1.73–1.70)
No. of reflections	174073	156441
No. of unique reflections	45852 (2304)	19187 (943)
Multiplicity	3.8 (3.8)	8.2 (8.3)
Mean $I/\sigma(I)$	32.5 (4.2)	33.8 (5.5)
Completeness (%)	98.7 (99.6)	99.3 (98.8)
R_{merge} (%)	7.3 (44.5)	8.8 (43.2)
Wilson B factor (Å)	29.6	15.4
Refinement		
R_{work} (%)	18.8 (24.9)	16.9 (16.4)
R_{free} (%)	21.3 (27.5)	19.4 (20.5)
R.m.s.d., bond lengths (Å)	0.007	0.005
R.m.s.d., bond angles (°)	0.827	0.901
B factor (Å^2)		
Overall	26.1	18.7
Molecule A(B)	35.2 (35.2)	17.8
Water	42.6	28.9
No. of non-H atoms		
Protein (solvent)	3237 (483)	1602 (146)
Ramachandran statistics		
Favored (%)	98.2	98.5
Disallowed (%)	0	0.51
Rotamer outliers	0	0
PDB entry	6L1D	6L1M

The structures of mouse STARD4 [17], human STARD5 [5] and human STARD6 [18] were reported previously. Structural comparison shows that the structural folds of the STARD4 subfamily members are well conserved with the pairwise C_α RMSD of less than 2.0 Å (Fig. 2B). However, the residues forming the cavity walls are not highly conserved with the sequence identities of 40–53% between STARD4 and STARD5/6, implying variation of sterol recognition in these members [19]. The core domains of human and mouse STARD4 excluding the N-terminal extension display almost identical backbone structures with C_α RMSD of 0.394 Å.

3.2. The closed conformation of the Ω1-loop

The structure of human STARD4 displays a closed conformation of the Ω1-loop. The Ω1-loop was ordered in the crystal with clear electron densities. The protruding end of the Ω1-loop has four hydrophobic residues. The side chains of Leu107, Ile110 and Ile111 form a hydrophobic contact with α4 and close the tunnel entrance (Fig. 2A). The bulky hydrophobic side chain of Tyr108 (Leu124 in mouse STARD4) at the tip of the Ω1-loop is fully exposed to solvent. All members of the STARD4 subfamily has a hydrophobic residue at this position, which is critical for membrane interaction and sterol transport [16].

To examine the functional significance of the Ω1-loop, we constructed a deletion mutant (Δ107-110), in which the four Ω1-loop residues 107–110 (LWNI) were mutated to two glycine residues. The Δ107-110 mutant was soluble and purified as a homogenous monomer suggesting that the mutation does not interfere with protein folding. The structure of Δ107-110 mutant was solved at 1.7 Å resolution by molecular replacement (Fig. 2C). The Ω1-loop of the Δ107-110 mutant is two-residue shorter than the wild type (STARD4 C75S was referred as wild type in this manuscript). The Ω1-loop of the Δ107-110 mutant had a closed conformation and was well-ordered in the crystal structure. Gln106 and Ser112 make hydrogen bonds with Thr193 (α4) and Arg114 (β6), respectively, stabilizing the closed conformation of the lid. Ile111 forms a hydrophobic contact with the base of α4 closing the tunnel entrance. The overall structure of the Δ107-110 mutant was almost identical to the wild type. However, the Ω1-loop region and helix α4 had a conformational difference. Owing to the absence of Leu107 and Ile110 in the mutant, the hydrophobic contact between the Ω1-loop and α4 was reduced, which seems to induce a conformational change of α4. The N-terminal half of α4 in the Δ107-110 mutant was retracted toward the center by 1.6 Å compared to the wild type. This finding suggests that the hydrophobic residues (LWNI) in the Ω1-loop is not only critical for membrane binding but also influence the conformation of helix α4. The structural difference might represent a conformational flexibility of the Ω1-loop and helix α4 required for the open/closure of the pocket during lipid transfer cycles.

3.3. A conformational change of the Ω1-loop required for sterol-binding

The structure determination of a sterol-bound STARD is essential for understanding how a STARD domain recognizes cholesterol. So far, the structures of sterol-binding STARD homologs (STARD1/3/4/5/6) were determined only in apo-forms. We tried to obtain a cholesterol-bound structure of human STARD4 by incubating the protein with excess amounts of cholesterol. However, crystallographic analysis of the crystals grown in the presence of cholesterol showed only apo STARD4 with a closed conformation. It was proposed that cholesterol binds its 3-hydroxy group oriented to the center of the cavity and might form a hydrogen bond with a hydrophilic residue in the cavity wall in the STARD4 subfamily members [7,20]. Molecular dynamics simulations of STARD3 suggested that the movement of the Ω1-loop would be sufficient to allow sterol binding and release [21].

Structural analysis of the human STARD4 suggests that a conformational change involving the Ω1-loop seems to be essential

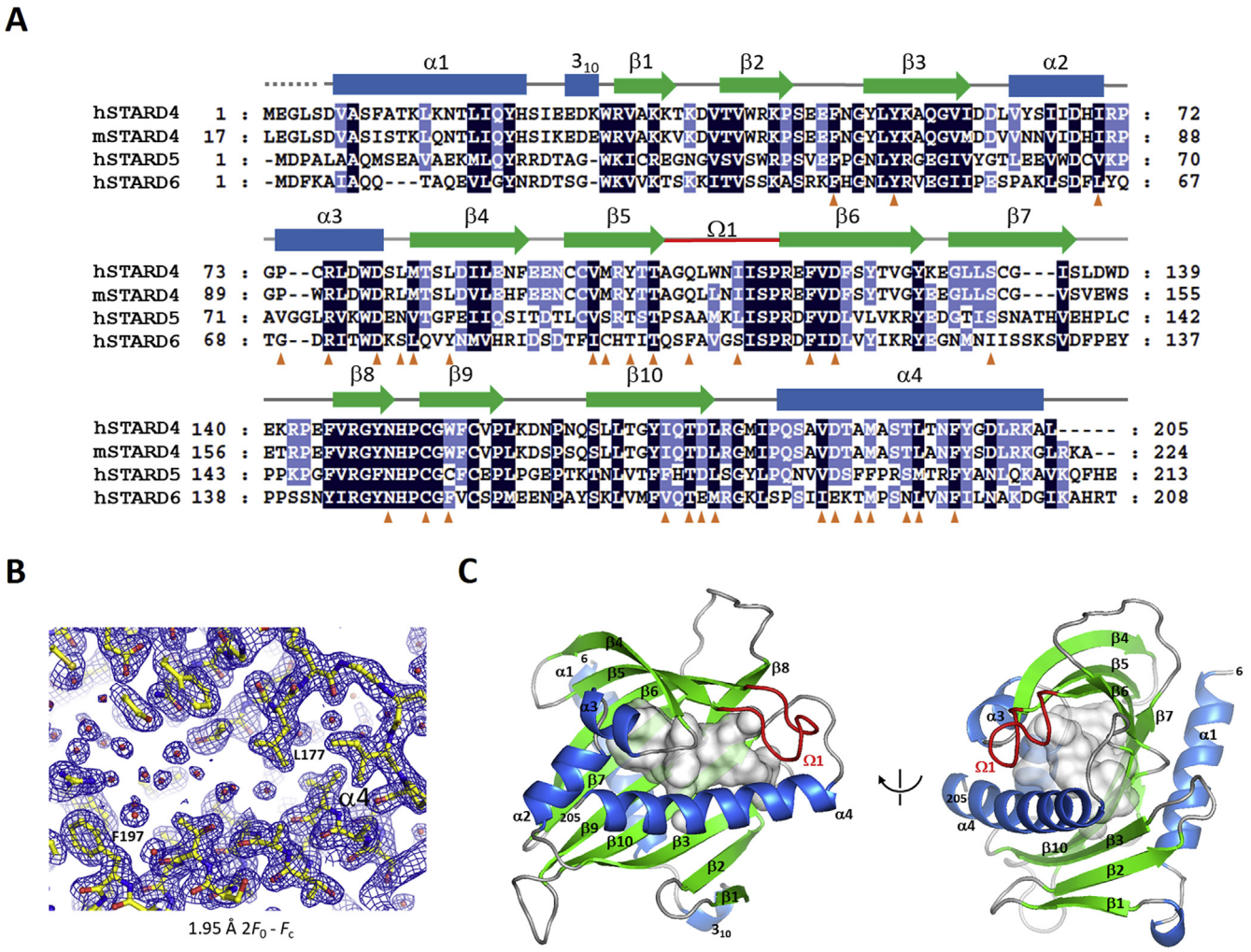

Fig. 1. Overall structure of human STARD4. (A) Sequence alignment of the human and mouse STARD4/5/6. The secondary structure elements for human STARD4 are shown on the top. The conserved residues are shaded in dark and light blue depending on the conservation. The orange arrows indicate the residues composing the wall of the sterol-binding pocket. (B) 1.95 Å $2F_0$-F_c electron density maps of human STARD4 C75S with the final model superimposed. (C) Overall structure of human STARD4. The Ω1-loop is colored in red. The sterol-binding cavity is shown in surface representation. The cavity was analyzed and prepared by GetCleft plugin (http://biophys.umontreal.ca/nrg/resources.html) in PyMOL (For interpretation of the references to color in this figure legend, the reader is referred to the Web version of this article.)

for sterol-binding. The total cavity volume (642 Å^3) of human STARD4 is larger than the volume of cholesterol (432 Å^3). However, the shape of the sterol-binding pocket in the closed form is not compatible for sterol-binding (Fig. 2D). The longest dimension of the major binding pocket is 4 Å shorter than cholesterol. In addition, the center of the binding pocket is too narrow to contain a sterol molecule. This finding suggests that a conformational change must accompany ligand binding. Considering the rigidity of the core α-helix/β-grip fold and the flexibility of the Ω1-loop in STARD domains, a partial opening of the Ω1-loop upon sterol-binding seems to be most probable based comparison with the sterol-binding mode of the related LAM StARkin domains (Fig. 2E) [12].

3.4. Sterol transport activity of human STARD4

We examined sterol transfer activity of the purified human STARD4 between liposomes. Dehydroergosterol (DHE) is a fluorescent sterol with the excitation and emission wavelengths of 324 nm and 375 nm, respectively. We prepared DHE/DOPC as a sterol donor liposome and Dansyl-PE/DOPC as an acceptor liposome. The transport of DHE to the acceptor liposomes results in close proximity of DHE and Dansyl-PE, which allows fluorescence resonance energy transfer (FRET) between the molecules. When STARD4 protein was added to the mixture of donor/acceptor liposomes, we observed an immediate increase of fluorescence at 525 nm generated by the FRET between DHE and Dansyl-PE (Fig. 3A). However, when non-fluorescent ergosterol was included in the DHE/DOPC donor liposomes, the FRET signal was reduced suggesting that ergosterol was competing with DHE for STARD4 binding (Fig. 3A). The data clearly indicate that STARD4 transported the DHE in the donor liposomes to acceptor liposomes. In the sterol transport assay, the DHE transport reached to the equilibrium in 200s indicating that human STARD4 transports efficiently between liposomes. The sterol binding to the hydrophobic cavity is an essential process in sterol transfer cycles. The mutations (I173Y and T175Y) in the hydrophobic walls of the sterol-binding cavity completely abolished the transfer activity, indicating that the complementary hydrophobic interaction with the cavity wall is essential for sterol transport (Fig. 3B). The mutations around the tunnel entrance, L82A in the α3−β4 and T193L of α4, reduced the

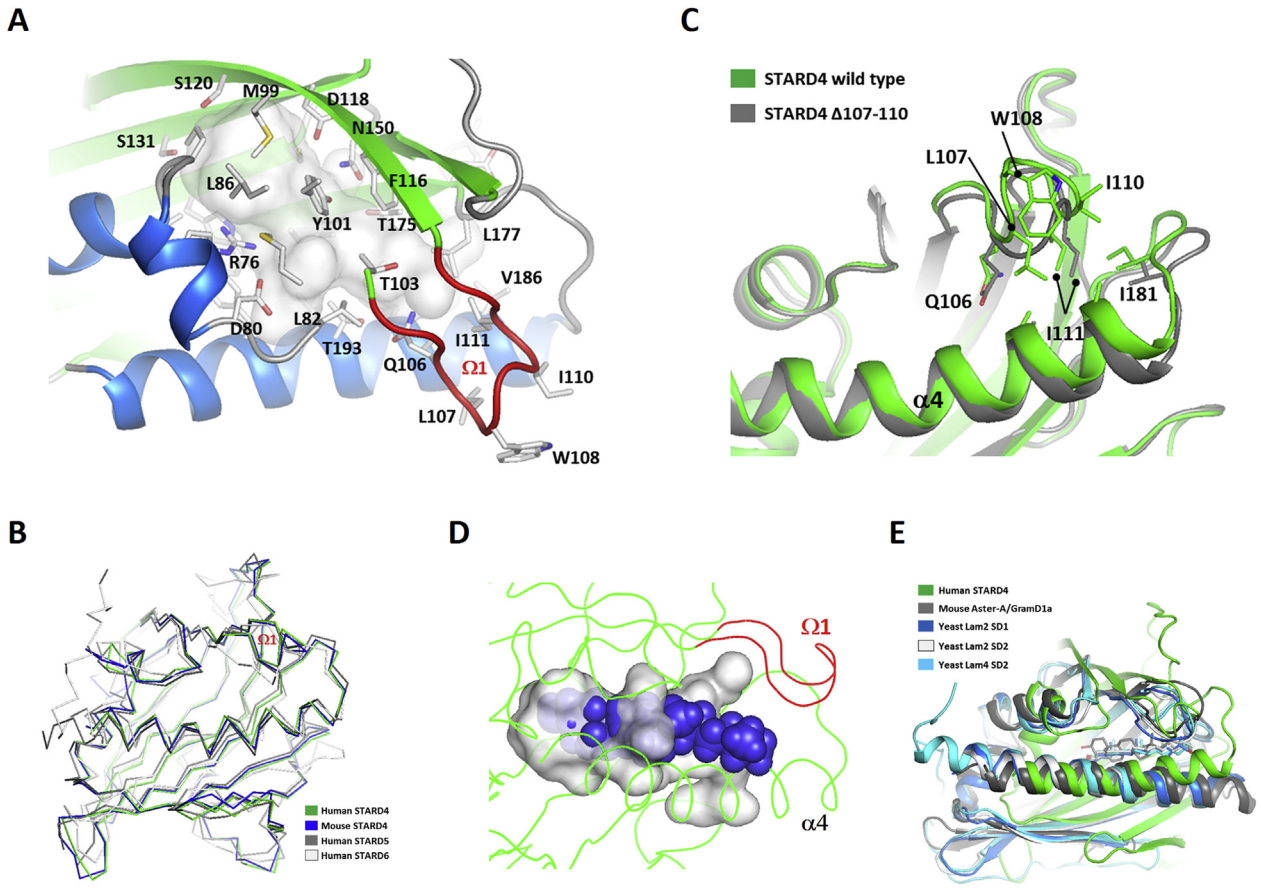

Fig. 2. Sterol-binding pocket. (A) The residues composing the wall of sterol binding cavity are shown in sticks. (B) Superposition of human and mouse STARD4/5/6 structures. Mouse STARD4 (PDB id: 1JSS) human STARD5 (PDB id: 2R55), human STARD6 (PDB id: 2MOU). (C) Structural comparison of the STARD4 wild type and the Δ107-110 mutant. (D) Sterol binding cavity of human STARD4. The cholesterol in the sterol-binding pocket was modeled in based on the structural comparison with the LAM StARkin structures. Hydrogen atoms were included in the sphere model of cholesterol. The sterol-binding cavity of human STARD4 is shown in a transparent surface. (E) Superposition of human STARD4 with the sterol-bound structures of the LAM StARkin domains (Aster-A PDB id: 6GQF [22], Lam2 SD1 PDB id: 6CAY [13], Lam2 SD2 PDB id: 5YS0 [12], Lam4 SD2 PDB id: 6BYM [14]).

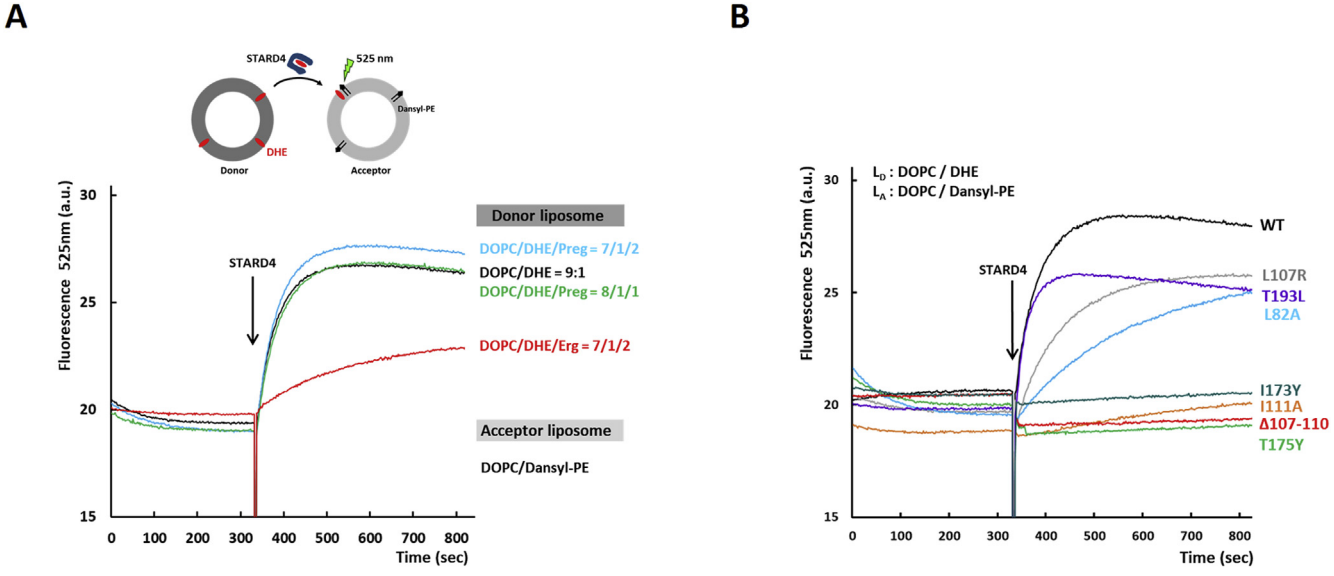

Fig. 3. Sterol transport by human STARD4. (A) DHE transport assay between liposomes by the human STARD4. DOPC/DHE (90/10 mol/mol) and DOPC/Dansyl-PE (97.5/2.5) liposomes were mixed at 25 °C. After 320 s, human STARD4 (1 μM) was added. FRET between DHE and Dansyl-PE was monitored as DHE is transported to the acceptor liposomes. Preg and Erg denote pregnenolone and ergosterol, respectively. (B) DHE transport by the human STARD4 and its mutants. L_D and L_A indicate donor liposomes and acceptor liposomes, respectively.

transfer activity more than 30%. The L107R mutation of the Ω1-loop reduced transfer activity. The Δ107-110 and I111A mutations of the Ω1-loop completely abolished transfer activity. These data are consistent with the previous studies indicating the key role the Ω1-loop in sterol transport [16].

A previous structural analysis on the STARD4 subfamily members suggested that smaller sterols such as steroids might be potential ligands considering small cavity volumes [19]. STARD6 was discovered to bind specifically testosterone as well as cholesterol [18]. We examined whether STARD4 can transport a small steroid, pregnenolone. Addition of pregnenolone in the DHE donor liposomes did not affect the DHE transport by STARD4, suggesting that pregnenolone did not compete with DHE and was not transported by STARD4 (Fig. 3A).

4. Discussion

Non-vesicular transport of sterol by STARD proteins serves as one of the major mechanisms for intracellular sterol distribution. Elucidating the structural mechanism of sterol recognition and transport by STARD proteins is important for understanding sterol homeostasis and processing. However, understanding the mechanism of sterol recognition has been complicated by the lack of structure of a sterol-bound form and by the variation of cavity size and shape between the homologs. Cholesterol is predicted to bind to the pocket in a head-down orientation with its hydrophobic acyl group located toward the tunnel entrance [7]. The structure of STARD4 with a closed lid does not display a shape complementarity of the pocket to cholesterol. The insufficient size of the hydrophobic pocket of human STARD4 suggested that a conformational change involving the Ω1-loop is essential for sterol-binding. We observed that the conformation of helix α4 is affected by the hydrophobic interaction with the Ω1-loop, which is consistent with the previous study that sterol binding to STARD6 involves the conformational change of the Ω1-loop and N-terminal portion of α4 [18]. The cavity volumes of STARD4 subfamily proteins were estimated to be 308–535 $Å^3$, which is similar to or slightly smaller than the volume of sterol ligands [19]. Recent structural analysis of sterol-bound StARkin domains revealed that the hydrophobic interaction with surface complementarity is a critical factor for sterol binding and that the conformational change upon sterol binding is limited to the Ω1-loop [12–14,22]. Sterol does not occupy the bottom of the hydrophobic cavity, rather it binds closely to the tunnel entrance of the LAM StARkin domains with the partially open Ω1-loop conformation. The exact mechanism of STARD4 recruitment to membranes is not fully understood. The mutation of the Ω1-loop of mouse STARD4 resulted in a large reduction in the level of membrane interaction and sterol transfer activity [4]. STARD4 has a surface patch of conserved basic residues in β1 and β2 and a nonpolar Ω1-loop. The basic patch is important for the membrane interaction and sterol transfer by interacting with anionic lipids, such as phosphatidylserine [10,16].

In conclusion, this study confirms the structural conservation of the STARD4 subfamily proteins and the significance of the Ω1-loop in sterol transport. Sterol transfer assays suggested that the major force of sterol binding is complementary hydrophobic interaction. To accommodate a sterol molecule in the pocket, a conformational change involving a partial opening of the Ω1-loop seems to be accompanied, which might form a complementary pocket to cholesterol.

Accession numbers

The coordinates and structure factors of hSTARD4 C75S and the Δ107-110 mutant have been deposited in the Protein Data Bank with the accession codes, 6L1D and 6L1M, respectively.

Declaration of competing interest

The authors declare no conflict of interests.

Acknowledgements

This project was supported by the National Research Foundation of Korea (NRF) grant funded by the Ministry of Education, Science and Technology (grant no.2017R1A2B4004914).

Transparency document

Transparency document related to this article can be found online at https://doi.org/10.1016/j.bbrc.2019.10.054.

Appendix A. Supplementary data

Supplementary data to this article can be found online at https://doi.org/10.1016/j.bbrc.2019.10.054.

References

[1] G. van Meer, D.R. Voelker, G.W. Feigenson, Membrane lipids: where they are and how they behave, Nat. Rev. Mol. Cell Biol. 9 (2008) 112–124.
[2] L. Liscum, N.J. Munn, Intracellular cholesterol transport, Biochim. Biophys. Acta 1438 (1999) 19–37.
[3] D.B. Iaea, S. Mao, F.W. Lund, F.R. Maxfield, Role of STARD4 in sterol transport between the endocytic recycling compartment and the plasma membrane, Mol. Biol. Cell 28 (2017) 1111–1122.
[4] L.H. Wong, A.T. Gatta, T.P. Levine, Lipid transfer proteins: the lipid commute via shuttles, bridges and tubes, Nat. Rev. Mol. Cell Biol. 20 (2019) 85–101.
[5] A.G. Thorsell, W.H. Lee, C. Persson, M.I. Siponen, M. Nilsson, R.D. Busam, T. Kotenyova, H. Schuler, L. Lehtio, Comparative structural analysis of lipid binding START domains, PLoS One 6 (2011), e19521.
[6] F. Alpy, C. Tomasetto, Give lipids a START: the StAR-related lipid transfer (START) domain in mammals, J. Cell Sci. 118 (2005) 2791–2801.
[7] Y. Tsujishita, J.H. Hurley, Structure and lipid transport mechanism of a StAR-related domain, Nat. Struct. Biol. 7 (2000) 408–414.
[8] D. Rodriguez-Agudo, S. Ren, P.B. Hylemon, K. Redford, R. Natarajan, A. Del Castillo, G. Gil, W.M. Pandak, Human StarD5, a cytosolic StAR-related lipid binding protein, J. Lipid Res. 46 (2005) 1615–1623.
[9] H.S. Bose, R.M. Whittal, Y. Ran, M. Bose, B.Y. Baker, W.L. Miller, StAR-like activity and molten globule behavior of StARD6, a male germ-line protein, Biochemistry 47 (2008) 2277–2288.
[10] B. Mesmin, N.H. Pipalia, F.W. Lund, T.F. Ramlall, A. Sokolov, D. Eliezer, F.R. Maxfield, STARD4 abundance regulates sterol transport and sensing, Mol. Biol. Cell 22 (2011) 4004–4015.
[11] K.V. Tugaeva, N.N. Sluchanko, Steroidogenic acute regulatory protein: structure, functioning, and regulation, Biochemistry (Mosc.) 84 (2019) S233–S253.
[12] J. Tong, M.K. Manik, Y.J. Im, Structural basis of sterol recognition and nonvesicular transport by lipid transfer proteins anchored at membrane contact sites, Proc. Natl. Acad. Sci. U. S. A. 115 (2018) E856–E865.
[13] F.A. Horenkamp, D.P. Valverde, J. Nunnari, K.M. Reinisch, Molecular basis for sterol transport by StART-like lipid transfer domains, EMBO J. 37 (2018).
[14] J.A. Jentsch, I. Kiburu, K. Pandey, M. Timme, T. Ramlall, B. Levkau, J. Wu, D. Eliezer, O. Boudker, A.K. Menon, Structural basis of sterol binding and transport by a yeast StARkin domain, J. Biol. Chem. 293 (2018) 5522–5531.
[15] P. Sheffield, S. Garrard, Z. Derewenda, Overcoming expression and purification problems of RhoGDI using a family of "parallel" expression vectors, Protein Expr. Purif. 15 (1999) 34–39.
[16] D.B. Iaea, I. Dikiy, I. Kiburu, D. Eliezer, F.R. Maxfield, STARD4 membrane interactions and sterol binding, Biochemistry 54 (2015) 4623–4636.
[17] M.J. Romanowski, R.E. Soccio, J.L. Breslow, S.K. Burley, Crystal structure of the Mus musculus cholesterol-regulated START protein 4 (StarD4) containing a StAR-related lipid transfer domain, Proc. Natl. Acad. Sci. U. S. A. 99 (2002) 6949–6954.
[18] D. Letourneau, M. Bedard, J. Cabana, A. Lefebvre, J.G. LeHoux, P. Lavigne, STARD6 on steroids: solution structure, multiple timescale backbone dynamics and ligand binding mechanism, Sci. Rep. 6 (2016) 28486.
[19] D. Letourneau, A. Lefebvre, P. Lavigne, J.G. LeHoux, The binding site specificity of STARD4 subfamily: breaking the cholesterol paradigm, Mol. Cell. Endocrinol. 408 (2015) 53–61.
[20] D. Letourneau, A. Lefebvre, P. Lavigne, J.G. LeHoux, STARD5 specific ligand binding: comparison with STARD1 and STARD4 subfamilies, Mol. Cell. Endocrinol. 371 (2013) 20–25.

[21] M. Murcia, J.D. Faraldo-Gomez, F.R. Maxfield, B. Roux, Modeling the structure of the StART domains of MLN64 and StAR proteins in complex with cholesterol, J. Lipid Res. 47 (2006) 2614–2630.
[22] J. Sandhu, S. Li, L. Fairall, S.G. Pfisterer, J.E. Gurnett, X. Xiao, T.A. Weston, D. Vashi, A. Ferrari, J.L. Orozco, C.L. Hartman, D. Strugatsky, S.D. Lee, C. He, C. Hong, H. Jiang, L.A. Bentolila, A.T. Gatta, T.P. Levine, A. Ferng, R. Lee, D.A. Ford, S.G. Young, E. Ikonen, J.W.R. Schwabe, P. Tontonoz, Aster proteins facilitate nonvesicular plasma membrane to ER cholesterol transport in mammalian cells, Cell 175 (2018) 514–529 e520.